CHARACTERIZATION OF POLYMER POWDERS FOR SELECTIVE LASER SINTERING

J. Schmidt*‡, M. A. Dechet*‡, J. S. Gómez Bonilla*‡, N. Hesse*‡, A. Bück*‡, W. Peukert*‡

* Institute of Particle Technology, Friedrich-Alexander-Universität Erlangen-Nürnberg, Cauerstraße 4, D-91058 Erlangen, Germany

‡ Collaborative Research Center 814 – Additive Manufacturing, Friedrich-Alexander-Universität Erlangen-Nürnberg, Am Weichselgarten 6, D-91058 Erlangen, Germany

Abstract

Flowability and packing properties are essential for powder spreading and resulting part properties in powder bed fusion processes (PBF), such as selective laser sintering (SLS). In this contribution, powder requirements for SLS, structure-property relationships and appropriate methods for powder characterization are reviewed. Effects of particle size, particle shape and surface functionalization on flowability, packing density and tribo-charging will be discussed for commercial PA12 laser sintering powders (virgin vs. aged), polyolefin and polyester powders. The possibilities of dry particle coating as an efficient method to tailor powder flowability, bulk density and charging behavior are demonstrated. The capabilities of a Schulze ring shear tester, a powder tensile strength tester, a thermally controllable ring shear apparatus and a model experiment mimicking the powder spreading are discussed to assess SLS processability.

Introduction

Powder bed fusion processes (PBF), such as e.g. selective laser sintering (SLS) / laser sintering (LS), selective laser melting (SLM) or selective electron beam melting (SEBM), allow for manufacture of complex functional parts without the need for any tools or molds. Briefly, in these processes the part is built layer by layer from powders, which are selectively melted. In SLS, a thermoplastic powder –preferentially a semi-crystalline polymer, mostly polyamide 12 (PA12)- is selectively melted by a laser (typically CO_2, 10.6 μm wavelength): The manufacture is performed in SLS machines in a building chamber, which is typically heated to a process temperature slightly below the melting temperature of the respective polymer feed powder –in case of PA12 around 167 °C. First, the powder material is applied at a certain powder layer thickness (typically 100 μm to 150 μm) to the building platform by means of a spreading unit, which frequently is either a rake or a roller coater. Then, the applied powder is selectively melted, where the later (solid) part is desired. Finally the building platform is lowered by around one powder layer thickness and a new building cycle starts with the powder spreading step. From this short sketch of the SLS process it already becomes obvious, that there are many factors that will affect processability and part quality in terms of e.g. dimensional accuracy and mechanical properties. Factors that influence SLS processability have been intensively discussed in literature (c.f. e.g. [1-5]) and are summarized in the scheme depicted in Figure 1. One can subdivide factors that determine SLS processability into intrinsic material properties and (extrinsic) bulk solid properties. Intrinsic material properties, like optical, thermal (melting temperature, solidification temperature, degree of crystallinity, heat capacity, thermal expansion coefficient) or rheological properties (melt viscosity) depend on the formulation of the plastic, i.e. type of polymer and its structure, the molar mass distribution, cross-linking, additive enhancement. The given material characteristics influence for example the so-called sintering window, which can be employed during PBF of polymers, i.e. the temperature difference between onset of melting and onset of solidification temperature or the melting and melt coalescence behavior and, thus, are e.g. important to identify proper building chamber temperature or energy input during laser illumination [6]. The extrinsic properties of the polymer powder, i.e. its bulk solid properties like flowability, packing characteristics (c.f. bulk vs. tapped density) depend mainly on inter particulate interactions, which are determined for example by the particle size distribution, the particle shape or the particle surface characteristics (surface roughness, surface chemistry). The mentioned particle characteristics are a function on the processes applied for particle formation and / or functionalization.

Within this account we will review techniques that allow for characterization of extrinsic SLS material properties, i.e. bulk solid and particle characteristics. Moreover, pathways for modification of powder systems for improvement of SLS processability will be exemplified.
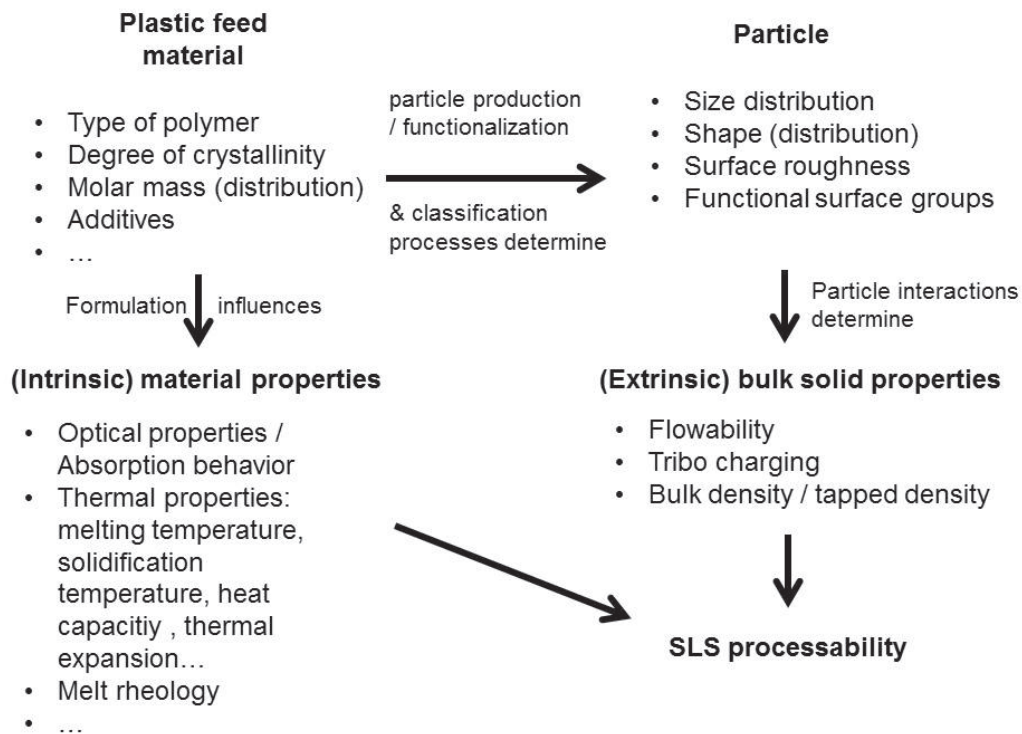

Figure 1: Overview on key characteristics of thermoplast powders influencing processability in selective laser sintering (SLS).

Bulk solid characteristics of commercial SLS powders

Most of the currently employed SLS powder by market share (> 90 %) is made up of polyamides (PA), mainly polyamide 12 (PA12) besides some PA11 and PA6. The PA12 materials are available as a standard grade but also as special grades e.g. enhanced with flame retardants or as glass, carbon or aluminum filled systems. PA particle systems for SLS typically are produced either by direct polymerization (c.f. Orgasol grades by Arkema) or precipitation (c.f. e.g. PA2200 (EOS) or DuraForm PA (3D Systems)). Besides PA powders, there are commercial SLS powders made up of polystyrene (PS), polypropylene (PP), thermoplastic eleastomers (TPE) or polyether ether ketone (PEEK) available [4-9]. For further information on commercial SLS particle systems and recent developments, please refer e.g. to [8] or [4]. SLS polymer powders also can be obtained by cryogenic grinding (c.f. PA1101 (EOS)), however, there can be issues with inferior flowability due to edged particle shapes being typical for comminution products [10] and, in consequence, inferior processability [11]. Commercial PA12 SLS powders of good processability typically have particle sizes between 45 µm and 90 µm. Moreover, they are often surface-functionalized with flowing aids (e.g. pyrogenic silica or alumina), which increases surface roughness and allows for minimization of particle interactions and, thus, improvement of flowability and packing density [12-18]. Figure 2 exemplarily depicts SEM pictures of PA2200 (EOS), a PA12 SLS powder. The particle shape (Figure 2, left), which is often referred to as 'potato-shape', is typical for polymer particles produced by precipitation, more precisely liquid-liquid phase separation and subsequent crystallization (for details on this process, please refer to our recent work [18]).
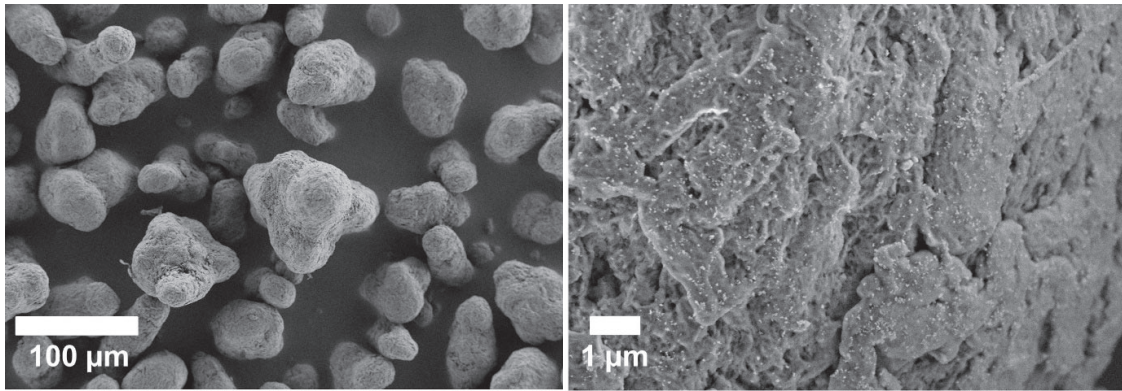
Figure 2: Scanning electron microscopic (SEM) pictures of PA12 SLS powder PA2200 (EOS). Left: 'potato-shaped' particles being typical for precipitated particles. Right: particle surface with flowing aid.

The surface functionalization of PA2200 with flowing aid becomes obvious from the material contrast being visible in Figure 2, right. Furthermore, the PA2200 particles are characterized by a rather narrow particle size distribution with $x_{10,3}$ = 45.8 μm, $x_{50,3}$ = 61.4 μm, $x_{90,3}$ = 81.0 μm and a span (($x_{10,3}$ - $x_{90,3}$)/ $x_{50,3}$) of 0.57. Narrow particle size distributions and the absence of fines is advantageous with respect to flowability and dense packing. To summarize, the key to optimization of PBF processability concerning bulk solid properties is control of

(i) particle shape (rounded particle shapes are advantageous)
(ii) particle size distribution (narrow distribution is advantageous)
(iii) particle surface roughness (rough particles allow for reduction of inter particulate forces and, thus, better flowability).

Strategies to achieve these goals will be discussed in the following section in line with methods for characterization of powder flowability and spreadability.

Methods for characterization of powder flowability

The determination of bulk solid properties at ambient temperature frequently already allows for a first assessment of the processability of the PBF material under process conditions. Powders of good flowability are essential, they typically show good spreadability during the powder deposition step and, thus, guarantee a dense and homogeneous powder layer and, consequently, parts of low porosity [9, 19, 20]. Various methods have been proposed so far, although there is no consensus, which method is most appropriate with respect to mimicking the stress conditions during powder spreading and, thus, reliable prediction of PBF processability.

Hausner ratio and Carr index

Frequently, as a rough estimate of flowability, the so-called Hausner ratio (HR) or the Carr index (C) are applied, see equations 1 and 2. Both aforementioned quantities describe the compressibility of powders, respectively, cohesion via the (non-consolidated) bulk density, ρ_{bulk}, and the tapped density, ρ_{tapped}.

$$HR = \frac{\rho_{tapped}}{\rho_{bulk}} \tag{1}$$

$$C = 100 \cdot \frac{\rho_{tapped} - \rho_{bulk}}{\rho_{tapped}} \tag{2}$$

The determination of these ratios seems rather straightforward and simple at a first glance, and, thus these flowability indicators are often used, although, there are some drawbacks: neither HR nor C are a direct measure for flowability, although, good flowability often correlates with low compressibility (c.f. Table 1). Moreover, bulk density and tapped density highly depend e.g. on the mode of filling a measurement cylinder for determination of the volume occupied by the bulk solid, or the mode of consolidation during tapping (tapping frequency, stroke, number of taps etc.) [21]. Thus, the obtained results may show a rather large variance, especially if no automated tapper devices are employed, i.e. if the powder consolidation instead is done

manually. However, these methods are among the few standardized flowability measurement procedures, which fuels their widespread application, despite their flaws.

Shear testers

Shear testers, like e.g. a ring shear cell, allow for the determination of powder flowability under well-defined conditions [16, 18, 22] and, thus, the comparison of the flowability of different materials via the flow function ffc. The flow function is given as the ratio of consolidation stress σ_1 and unconfined yield strength σ_c, see equation 3. The quantities σ_1 and σ_c are determined via construction of two Mohr stress circles.

$$ffc = \frac{\sigma_1}{\sigma_c} \tag{3}$$

Further details on the measurement procedure and shear cell geometry can be found e.g. in [16]. An assignment of flowability, flow function ffc (and Hausner ratio, HR) is given in Table 1. Figure 3 exemplifies flow functions determined for PA11 PBF materials at ambient temperature and demonstrates how flowing aids and the removal of fines help to improve powder flowability.
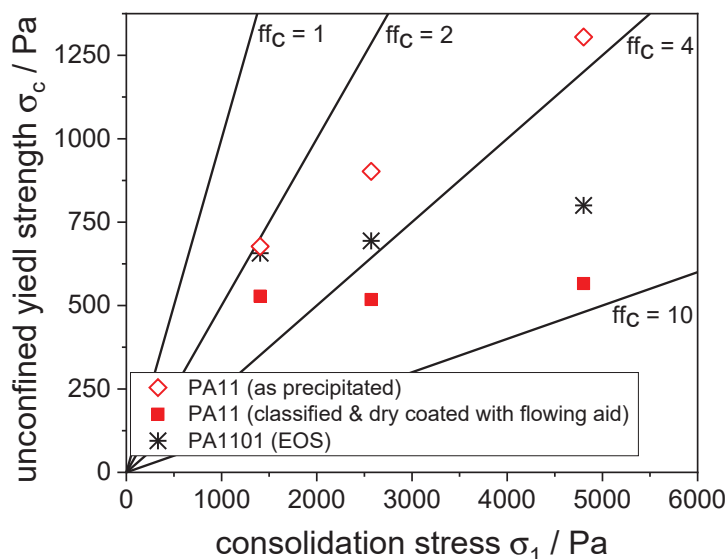

Figure 3: Flowability of PA11 powders as determined by shear experiments using a Schulze ring shear tester: narrowing of particle size distribution and dry coating with flowing aids allow to tune flow behavior from cohesive (2 < ffc < 4, red open symbols) to easy flowing (ffc > 4, red filled squares). The flow function ffc of commercial PA1101 (EOS) PBF material is given for reference.

The red open symbols depict the flow function of a PA11 powder obtained by liquid-liquid phase separation and (isothermal) precipitation of an injection molding grade Rilsan PA11 (Arkema) from ethanol at 120 °C and 20-wt.% polymer concentration. The process for particle production is outlined in great detail in [18]. The as-obtained powder after precipitation is characterized by a volume-averaged particle size of $x_{50,3} = 90$ µm and a $x_{10,3}$ of 27 µm and a $x_{90,3}$ of 185 µm. The particle size distribution (PSD) is rather broad, as expressed by the span $(x_{90,3} - x_{10,3}) / x_{50,3}$ of the PSD of 1.76. This material behaves cohesive (2 < ffc < 4). For improvement of flowability, the PSD was narrowed by sieving and the sieved PA11 powder with $x_{10,3} = 34$ µm, $x_{50,3} = 84$ µm, $x_{90,3} = 165$ µm (span = 1.56) was dry coated with 0.5 wt.-% of hydrophobic fumed silica, c.f. red filled squares in Figure 3: the classified and functionalized powder now is easy flowing (ffc >4, HR = 1.21). Dry coating of micron-sized host particles with flowing aids (nano-sized guest particles) is a well-known approach to increase powder flowability [15, 17, 18, 23]. Briefly, the nanoscale guest particles act as spacers between the micron-sized host particles and, thus, reduce particle-particle interactions by lowering the van der Waals adhesion forces [14, 24, 25] being highly dependent on interparticulate distance.

While shear testers allow for a well-reproducible determination of flowability, there is some criticism in using the obtained flow functions ffc for assessment of PBF processability, as ffc in shear testers typically is determined at rather high consolidation stresses that do not apply during powder spreading. Moreover, the

flowability of a pre-consolidated bulk solid is determined, which does not resemble the situation prior to powder spread in SLS machines. For example, if a rake is used for powder deposition, typically a non-consolidated bulk solid is spread; also if a roller coated is used, the bulk solid is applied as non-consolidated powder and the consolidation stress is rather low.

classification	Flow function ffc / -	Hausner ratio HR / -
non-flowing	< 1	
very cohesive	1 … 2	> 1.4
cohesive	2 … 4	1.25 … 1.4
easy-flowing	4 … 10	1.1 … 1.25
free-flowing	> 10	< 1.1

Table 1: Assignment of powder flowability: flow function ffc vs. Hausner ratio (HR) [21, 26].

Powder tensile tester

One approach to determine flowability of non-consolidated powders is the determination of the powder tensile strength. The measurement principle is outlined in the sketch given in Figure 4, left and described in our previous work, e.g. [10, 23]. A photograph of the powder tensile tester is depicted in Figure 4, right. The main components of the powder tensile tester are a powder reservoir, which is mounted on a motorized stage allowing for movement in vertical direction, a force transducer connected to a stamp that is moved into the powder reservoir and soft- and hardware that allows for force measurement data acquisition. First, the powder to be measured is prepared as non-consolidated bulk solid, which can be achieved by sieving the powder into the reservoir and the powder surface is smoothed by a rake. Then, the powder reservoir is moved towards the stamp being mounted on a traverse connected to the force transducer and covered with a thin layer of adhesive (to allow for adhesion of the powder particles in the uppermost layer), see Figure 4, left. Upon contact with the powder layer, the stamp (slightly) penetrates the bulk solid until a certain (pre-set) maximal force is reached. Then, the motorized stage is stopped, the movement direction of the stage is reversed and the maximum force F_{max} is registered. Due to the adhesive layer on the stamp of surface area A_{stamp}, the uppermost particle layer is 'glued' to the stamp surface, thus, when moving back the stamp, the bulk solid breaks between the uppermost and the neighboring powder layer. The layer adhesion force $F_{layer-layer}$ can be determined from the maximum force F_{max} corrected for the gravitational force $F_{gravity}$ due to the particle mass adhering to the stamp. The powder tensile strength σ_{powder} then is

$$\sigma_{powder} = \frac{F_{layer-layer}}{A_{stamp}} \qquad (4)$$

Powder tensile strength, thus, gives a direct measure of the adhesion force between neighboring powder layers starting from the non-consolidated bulk solid. Good flowability correlates with low interparticulate interactions, i.e. low powder tensile strength. An example for the application of powder tensile strength measurements for characterization of powders for PBF of polymers is given in Figure 5. There, tensile strengths determined for different polystyrene (PS) microparticles of comparable particle size distribution, namely comminuted, irregular shaped PS particles [27], thermally rounded PS particles and comminuted and rounded PS particles that have been subjected to dry particle coating with a flowing aid (fumed silica) [10] are given. The data nicely confirm that change of shape (thermal rounding) and application of flowing aids (lowering interparticulate forces) are feasible strategies for improvement of flowability of PBF materials.

While powder tensile strength gives information on particle interactions in the unconsolidated bulk under more or less static conditions, no insights into the powder spreading behavior under dynamic conditions are accessible by this approach. Here, besides powder rheometry, the rotational powder analyzer, funnel flow experiments, or powder spreading model experiments are an option [16, 17, 28].
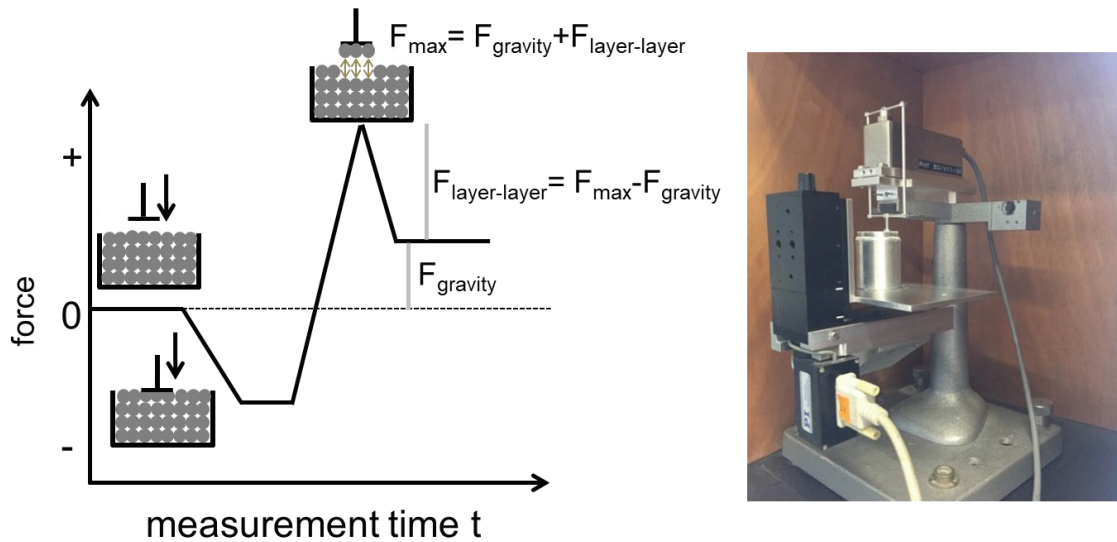
Figure 4: left: measurement principle of the powder tensile strength tester: (i) a stamp penetrates the non-consolidated bulk solid, (ii) the uppermost powder layer adheres to the stamp, (iii) the stamp is separated from the powder, the bulk solid breaks between adjacent layers and (iv) the interlayer adhesion force $F_{layer-layer}$ being a measure for flowability is accessible. Right: photograph of the powder tensile strength tester.
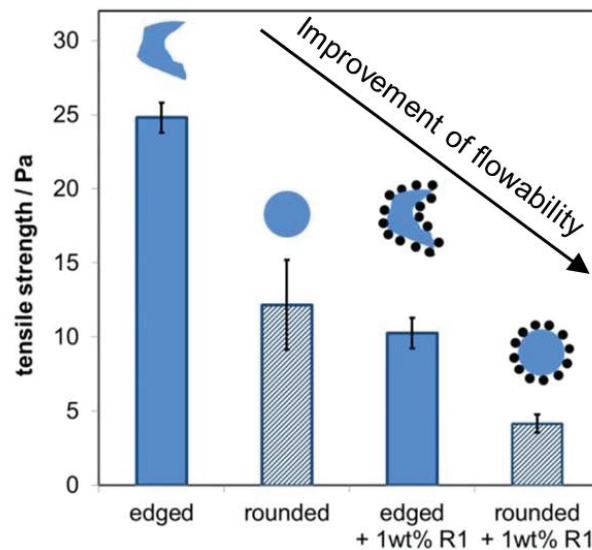

Figure 5: Effect of particle shape and surface functionalization on powder flowability as determined by powder tensile strength measurements: rounding of comminuted polystyrene (PS) particles and application of flowing aids by dry coating allows for reduction of interparticulate forces (reduction of powder tensile strength) and, thus, improvement of flowability [10].

Dynamic tests: revolution powder analyzer, powder rheometer, powder spreading experiments

For determination of flowability, different approaches have been discussed so far. For example, a so-called revolution powder analyzer has been proposed. The device consists of a rotating cylinder being equipped with transparent (circular) walls that allow for optical determination of the avalanche angle of the powder in dependency of the rotational frequency of the cylinder. Thus, this method allows for assessment of flow under stress conditions that are similar to that during powder spreading, if (circumferential) rotational speed is set close to the translational speed of the powder spreading unit [1, 3, 22, 29]. Moreover, for characterization of flowability under dynamic conditions, the measurement of the fluidization behavior of the PBF materials (c.f. minimum fluidization velocity), funnel flow experiments or so-called powder rheometers [30] have been

proposed. In the powder rheometer, the resistance of a bulk solid against flow is assessed via measurement of the acting torques during movement of a rotating blade fixed to a shaft. Depending on the mode of operation, the method allows for determination of cohesiveness and flowability, thus gives results that often correlate with HR or results from shear experiments. An extensive discussion and comparison of several methods can be found in the literature, e.g. [1, 3,22].

Different powder spreader model setups have been proposed so far. For example van der Eynde et al. [28] proposed a device that consists of a powder spreading unit (rake with variable, known gap size) and a load cell connected to a measurement plate (of known area), which –if the solid density of the material is known- allows for determination of the bulk density of the spread powder in dependence of e.g. gap height or spreader speed. Thus, this device allows for determination of a modified HR under powder spreading conditions (at ambient temperature). Powder spreading experiments on (typically black) model substrates with subsequent image analysis of the area covered with PBF material have been proposed to compare the spreadability of differently treated powders. For example, Blümel et al. [16] could show a good correlation between ffc determined by shear experiments, powder tensile strength, surface coverage with PBF material in the model powder spreading experiment and quality of laser sintered single layers for polyethylene powder coated with different flowing aids. Schmidt et al. [17] could prove an analogous behavior for polybutylene terephthalate (PBT) powders: powder tensile strength, surface coverage with PBT powder in spreading model experiments and quality of SLS single layer specimen show a strong correlation as depicted in Figure 6.
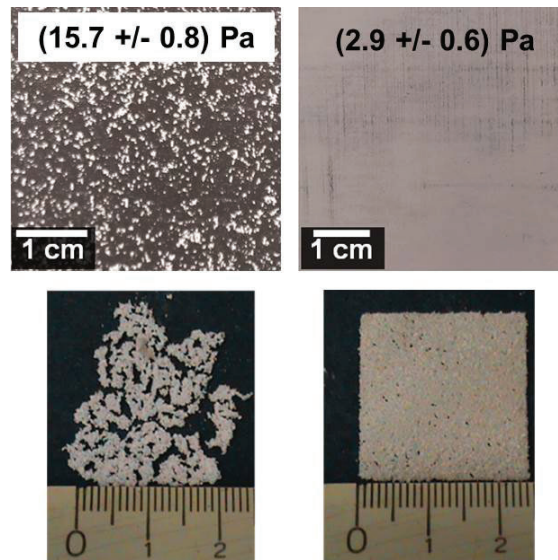

Figure 6: Effect of particle shape (ground (left) vs. rounded and dry coated (right) of PBT powders on powder tensile strength (insets, top), surface coverage in the model powder spreading experiment ((19.1 +/- 4.2) % vs. (97.3 +/- 1.8) %, comminuted vs. rounded and dry coated) and quality of SLS single layers (bottom) [17].

Tribo charging of PBF powders during powder spreading

A variant of the aforementioned powder spreading model setup has been recently proposed to assess the tribo charging of PA12 SLS powders of different ageing state during powder deposition. The model deposition experiments were performed at room temperature, the setup is depicted in Figure 7, top; the spreader unit has been complemented by a probe of an electrostatic voltmeter, that allows for measurement of surface potentials and, thus, surface charge. The electrostatic potential was monitored in dependence on position, the number of consecutive application steps and the ageing state of the powder. Figure 7, bottom depicts exemplarily results for an aged PA12 powder: tribo charging during powder deposition occurs and a charge accumulation, i.e. increase of potential and, thus, charge with increasing number of powder applications was noted. The charge built up also is a function of ageing state of the SLS material (virgin powder shows less tribo charging). A detailed discussion can be found in Hesse et al. [31].
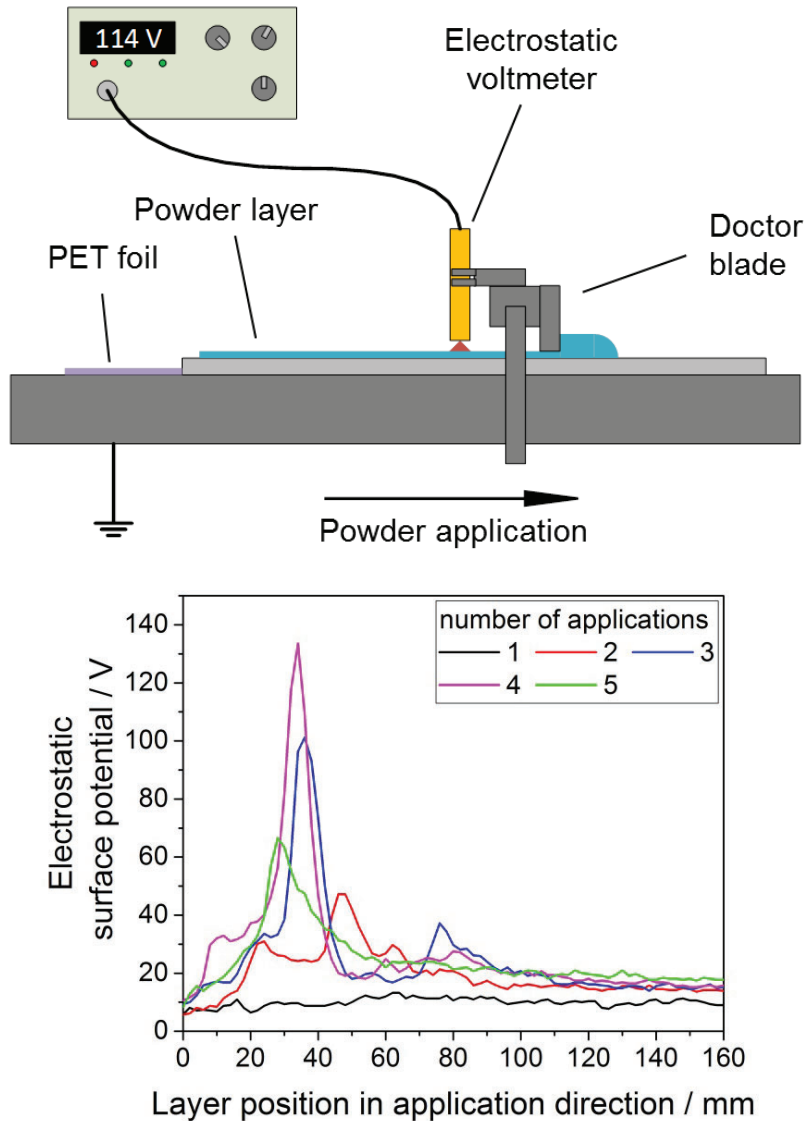
Figure 7: top: Model setup for determination of tribo charging during powder spreading; bottom: electrostatic surface potential during spreading of aged PA12 SLS powder [31].

Powder flowability at elevated temperatures

While, as outlined in the previous sections, there have been proposed many setups and measurement protocols to characterize powder flowability of PBF materials under different stress conditions, most of these experiments were performed at ambient temperature, i.e. little attention has been paid on the effect of temperature on flowability. The effect of temperature on powder flowability is far from being negligible, as powder spreading in SLS is performed at building chamber temperature, which e.g. in the case of PA12 typically is around 170 °C. Moreover, information on flowability at ambient conditions does not allow for an assessment of flowability at elevated temperature, as particle interactions, which determine powder flowability, can show complex and pronounced dependencies on temperature, as demonstrated in studies for organic matter (lactose, coffee, waxes) [32] or fly ashes [33, 34]. For example, adhesion forces can increase with increasing temperature due to changes in adsorption layers, liquid bridges, contact areas due to visco-plastic deformation, or flowability can decrease due to formation of solid bridges with beginning of sintering [32-38].

In a recent attempt, a (temperature-controlled) rheometer was modified with an appropriate measurement geometry that allows to perform shear experiments at elevated temperatures similar to the protocols employed in shear testers (see above). This is exemplified in Figure 8, which depicts the angle of internal friction φ_{sf} as

determined in dependency on temperature for virgin PA12 powder (PA2200, EOS). φ_{sf} is calculated from the shear stress τ and the normal stress via $\varphi_{sf} = arctan\,(\tau/\sigma)$. While steady state flow conditions are reached promptly for lower temperatures, at elevated temperatures τ does reach a maximum value and starts declining rapidly afterwards. Therefore the evaluated states for higher temperatures are at maximum shear stress as opposed to steady state conditions for lower temperatures. Obviously, a pronounced decrease of flowability is notable starting from around 150 °C up to a temperature close to the melting temperature of the polymer under consideration, as reflected by the increase by the increase in the angle of internal friction.
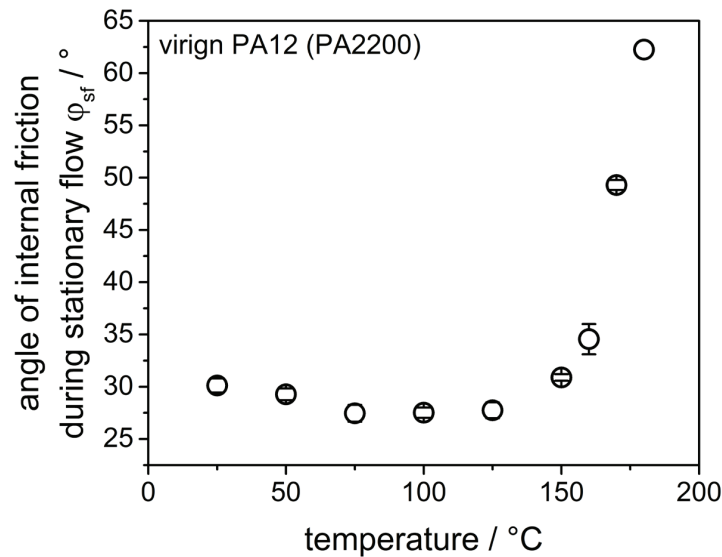

Figure 8: Temperature dependence of the angle of internal friction as determined for steady-flow conditions up to 150 °C and maximum shear stress above 150 °C for a PA12 SLS powder (PA2200, EOS).

Conclusions

In this contribution, different methods and experimental setups for assessment of bulk solid properties (flowability, packing density) relevant for processability of PBF materials were introduced and discussed. While the Hausner ratio (HR), i.e. the quotient of tapped density and (loose) bulk density, is frequently applied, one should keep in mind that the obtained results might be misleading, because HR is not a measure of powder flow, although for many materials a correlation of (small) HR and good flowability was found empirically. Moreover, the mode of powder consolidation and the measurement geometries can influence the result. Shear testers allow for reliable measurement of flowability (via the flow function ffc) under well-defined conditions; a positive correlation of large ffc value, small powder tensile strength and small HR was found for precipitated PA11 powder. Although, the stress conditions typically applied during the shear experiments are quite different from that during powder application. Consequently, powder spreading model experiments mimicking stress conditions during powder spreading are an alternative approach to characterize e.g. surface coverage with SLS powders or the tribo charging of the materials. The aforementioned characterization methods, so far, typically were performed room temperature. Characterization of flowability at process temperature, which can be quite different from that at ambient conditions, remains a challenge for future work.

Acknowledgements

Literature

[1]   A. Amado, M. Schmid, G. Levy, K. Wegener, Advances in SLS Powder Characterization, SFF Proceedings 2011, 438-452.

[2]   M. Schmid, A. Amado, K. Wegener, Journal of Materials Research 29 (2014) 1824-1832..

[3]   A. B. Spierings, M. Voegtlin, T. Bauer, and K. Wegener, Powder flowability characterisation methodology for powder-bed-based metal additive manufacturing, Progress in Additive Manufacturing, 1 (2016) 9-20.

[4]   S.Yuan, F. Shen, C. K. Chua, K. Zhou, Progress in Polymer Science 91 (2019) 141-168.

[5]   D. Bourell, J. P. Kruth, M. Leu, G. Levy, D. Rosen, A. M. Beese, A. Clare, Materials for additive manufacturing, CIRP Annals - Manufacturing Technology 66 (2017) 659-681.

[6]   C. A. Chatham, T. E. Long, C. B. Williams, A review of the process physics and material screening methods for polymer powder bed fusion additive manufacturing, Progress in Polymer Science 93 (2019) 68-95.[7]   R.D. Goodridge, C.J. Tuck, R. Hague, Laser sintering of polyamides and other polymers, Progress in Materials Science 57 (2012) 229–267.

[8]   T.T. Wohlers, Wohlers report 2016: 3D printing and additive manufacturing state of the industry annual worldwide progress report, Wohlers Associates, Fort Collins, Col., 2016.

[9]   M. Schmid, Selektives Lasersintern (SLS) mit Kunststoffen: Technologie, Prozesse und Werkstoffe, Hanser, München, 2015.[10]   J. Schmidt, M. Sachs, C. Blümel, B. Winzer, F. Toni, K.-E. Wirth,W. Peukert, A novel process route for the production of spherical LBM polymer powders with small size and good flowability, Powder Technology 261 (2014) 78–86.

[11] S. Berretta, O. Ghita, K. E. Evans, From polyamide to new PEEK powders, European Polymer Journal 59 (2014) 218-229.

[12] R. Pfeffer, R.N. Dave, D. Wei, M. Ramlakhan, Synthesis of engineered particulates with tailored properties using dry particle coating, Powder Technology 117 (2001) 40–67.

[13] H. Zhou, M. Götzinger, W. Peukert, The influence of particle charge and roughness on particle–substrate adhesion, Powder Technology 135-136 (2003) 82–91.

[14] M. Götzinger, W. Peukert, Particle Adhesion Force Distributions on Rough Surfaces, Langmuir 20 (2004) 5298–5303.

[15] J. Yang, A. Sliva, A. Banerjee, R.N. Dave, R. Pfeffer, Dry particle coating for improving the flowability of cohesive powders, Powder Technology 158 (2005) 21–33.

[16] C. Blümel, M. Sachs, T. Laumer, B. Winzer, J. Schmidt, M. Schmidt, W. Peukert, K.-E. Wirth, Increasing flowability and bulk density of PE-HD powders by a dry particle coating process and impact on LBM processes, Rapid Prototyping Journal 21 (2015) 697-704.

[17] J. Schmidt, M. Sachs, S. Fanselow, M. Zhao, S. Romeis, D. Drummer, K.-E. Wirth, W. Peukert, Optimized polybutylene terephthalate powders for selective laser beam melting, Chemical Engineering Science 156 (2016) 1–10.

[18] M. A. Dechet, A. Goblirsch, S. Romeis, M. Zhao, F. J. Lanyi, J. Kaschta, D. W. Schubert, D. Drummer, W. Peukert, J. Schmidt, Production of polyamide 11 microparticles for Additive Manufacturing by liquid-liquid phase separation and precipitation, Chemical Engineering Science 197 (2019) 11–25.

[19] M. Drexler, K. Wudy, D. Drummer, Einfluss des Pulverauftragsprozesses auf den selektiven Strahlschmelzprozess thermoplastischer Kunststoffe, RTejournal - Fachforum für Rapid Technologie (2015), urn:nbn:de:0009-2-42383.

[20] L. Verbelen, S. Dadbakhsh, M. van Den Eynde, J.-P. Kruth, B. Goderis, P. van Puyvelde, Characterization of polyamide powders for determination of laser sintering processability, European Polymer Journal 75 (2016) 163-174.

[21] E. Abdullah, D. Geldart, The use of bulk density measurements as flowability indicators Powder Technology 102 (1999) 151–165.

[22] S. Ziegelmeier, P. Christou, F. Wöllecke, C. Tuck, R. Goodridge, R. Hague, E. Krampe, E. Wintermantel, An experimental study into the effects of bulk and flow behaviour of laser sintering polymer powders on resulting part properties, Journal of Materials Processing Technology 215 (2015) 239–250.

[23] S. Fanselow, S.E. Emamjomeh, K.E. Wirth, J. Schmidt, W. Peukert, Production of spherical wax and polyolefin microparticles by melt emulsification for additive manufacturing, Chemical Engineering Science 141 (2016) 282–292.

[24] H. Rumpf, Mechanische Verfahrenstechnik, Carl Hanser Verlag, München - Wien, 1975.

[25] M. Götzinger, W. Peukert, Dispersive forces of particle–surface interactions: direct AFM measurements and modelling, Powder Technology 130 (2003) 102–109.

[26] D. Schulze, Powders and Bulk Solids, Behavior, Characterization, Storage and Flow, Springer, Berlin, 2008.

[27] J. Schmidt, M. Plata, S. Tröger, W. Peukert, Production of polymer particles below 5μm by wet grinding, Powder Technology 228 (2012) 84–90.

[28] M. van den Eynde, L. Verbelen, and P. van Puyvelde, Assessing polymer powder flow for the application of laser sintering, Powder Technology 286 (2015) 151–155.

[29] M. Krantz, H. Zhang, J. Zhu, Characterization of powder flow. Static and dynamic testing, Powder Technology, 194 (2009) 239–245.

[30] R. Freeman, Measuring the flow properties of consolidated, conditioned and aerated powders — A comparative study using a powder rheometer and a rotational shear cell, Powder Technology 174 (2007) 25–33.

[31] N. Hesse .M. A. Dechet, J. S. Gómez Bonilla C. Lübbert, S. Roth, A. Bück, J. Schmidt, W. Peukert, Analysis of Tribo-Charging during Powder Spreading in Selective Laser Sintering: Assessment of Polyamide 12 Powder Ageing Effects on Charging Behavior, Polymers 11 (2019), 609.

[32] Ripp, M.; Ripperger, S.: Influence of temperature on the flow properties of bulk solids, Chemical Engineering Science, 65 (2010) 4007–4013.

[33] Kamiya, H.; Kimura, A.; Yokoyama, T.; Naito, M.; Jimbo, G.: Development of a split-type tensile-strength tester and analysis of mechanism of increase of adhesion behavior of inorganic fine powder bed at high-temperature conditions, Powder Technology 127 (2002) 239–245.

[34] B. Zimmerlin, H. Leibold, H. Seifert, Evaluation of the temperature-dependent adhesion characteristics of fly ashes with a HT-rheometer,. Powder Technology 180 (2008) 17–20.

[35] C. Kanaoka, M. Hata, H. Makino, Measurement of adhesive force of coal flyash particles at high temperatures and different gas compositions, Powder Technology 118 (2001) 107–112.

[36] I. Tomasetta, D. Barletta, M. Poletto, The High Temperature Annular Shear Cell. A modified ring shear tester to measure the flow properties of powders at high temperature, Advanced Powder Technology 24 (2013) 609–617.

[37] T. Pilz, F. Löffler, Einfluß adhäsiver und kohäsiver Partikeleigenschaften bei der Filtration an Oberflächenfiltern,.Chemie Ingenieur Technik 67 (1995) 745–749.

[38] B. Formisani, R. Girimonte, L. Mancuso, Analysis of the fluidization process of particle beds at high temperature, Chemical Engineering Science 53 (1998) 951–961.